1 NO₃ chemistry of wildfire emissions: a kinetic study of the gas-phase
2 reactions of furans with the NO₃ radical

3 Mike J. Newland, Yangang Ren, Max R. McGillen, Lisa Michelat, Véronique Daële, Abdelwahid Mellouki

4 ICARE-CNRS, 1 C Av. de la Recherche Scientifique, 45071 Orléans Cedex 2, France

5

6 *Correspondence to*: Mike J. Newland (mike.newland@cnrs-orleans.fr; mellouki@cnrs-orleans.fr)

7

8

9 **Abstract.** Furans are emitted to the atmosphere during biomass burning from the pyrolysis of cellulose. They are one of the

10 major contributing VOC classes to OH and NO_3 reactivity in biomass burning plumes. The major removal process of furans

11 from the atmosphere at night is reaction with the nitrate radical, NO_3. Here we report a series of relative rate experiments in the

12 7300 L indoor simulation chamber at CNRS-ICARE, Orléans, using a number of different reference compounds to determine

13 NO_3 reaction rate coefficients for four furans, two furanones, and pyrrole. In the case of the two furanones, this is the first time

14 that NO_3 rate coefficients have been reported. The recommended values (cm^3 molecule^{-1} s^{-1}) are: furan $(1.50\pm0.23)\times10^{-12}$, 2-

15 methylfuran $(2.37\pm0.55)\times10^{-11}$, 2,5-dimethylfuran $(1.10\pm0.33)\times10^{-10}$, furan-2-aldehyde $(9.28\pm2.3)\times10^{-14}$, 5-methyl-2(3H)-

16 furanone $(3.00\pm0.45)\times10^{-12}$, 2(5H)-furanone $<1.4\times10^{-16}$, and pyrrole $(7.35\pm2.06)\times10^{-11}$. The furan-2-aldehyde + NO_3 reaction

17 rate is found to be an order of magnitude lower than previously reported. We also recommend a faster rate for the α-

18 terpinene+NO_3 reaction $((2.70\pm0.81)\times10^{-10}$ cm^{3}s$^{-1})$. These experiments show that for furan, alkyl substituted furans, 5-methyl-

19 2(3H)-furanone, and pyrrole, reaction with NO_3 will be the dominant removal process at night, and may also contribute during

20 the day. For 2(5H)-furanone, reaction with NO_3 is not an important atmospheric sink.

21 **1 Introduction**

22 Furans are five membered aromatic cyclic ethers. Furans (and pyrroles – where N replaces O as the heteroatom) are generated

23 during the pyrolysis of cellulose and are a major component of emissions from wildfire burning (Hatch et al., 2015, 2017; Koss

24 et al., 2018; Coggon et al., 2019; Andreae et al., 2019). Such emissions are likely to increase in the future with the spatial extent,

25 number, and severity, of wildfires globally having increased markedly in recent decades (Jolly et al., 2015; Harvey, 2016) and

26 predicted to continue to do so as the climate warms (Krikken et al., 2019; Lohmander, 2020). Furans have also been measured

27 in emissions from residential logwood burning (Hartikainen et al., 2018), and burning of a wide variety of solid-fuels used for

28 domestic heating and cooking (Stewart et al., 2021a). Furans have been shown to account for a significant proportion of the total

29 NO_3 (Decker et al., 2019) and OH (Koss et al., 2018; Coggon et al., 2019; Stewart et al., 2021b) reactivity of emissions from

30 burning of typical wildfire and domestic fuels.

31 Alkyl substituted furans have also been suggested as promising biofuels as they can be derived from lignocellulosic biomass

32 (Roman-Leshkov et al., 2007; Binder et al., 2009; Wang et al., 2014). This would likely lead to fugitive emissions of these

33 compounds during distribution, as well as emissions of unburned and partially oxidised products from vehicle exhaust. The

34 oxidation of certain furan compounds has been shown to have large secondary organic aerosol yields (Hatch et al., 2017;

35 Hartikainen et al., 2018; Joo et al., 2019, Ahern et al., 2019; Akherati et al., 2020), which could adversely impact air quality.

36 Oxidation of furans in the atmosphere has been shown to produce 2-furanones (mono-unsaturated five-membered cyclic esters)

37 both via OH (notably hydroxy-furan-2-ones, Aschmann et al., 2014) and NO_3 (Berndt et al., 1997) reactions. 2-Furanones are

38 also produced from the OH oxidation of six-membered aromatic compounds (Smith et al., 1998, 1999; Hamilton et al., 2005;
39 Bloss et al., 2005; Wyche et al., 2009; Huang et al., 2015). In both cases, the initial product is thought to be an unsaturated
40 dicarbonyl, with production of the 2-furanone formed via photoisomerisation of the dicarbonyl to a ketene-enol (Newland et al.,
41 2019), followed by ring closure of this molecule. In the case of aromatics, the ketene-enol can also be formed directly via
42 decomposition of the bicyclic peroxy radical intermediate (Wang et al., 2020).

43 Furan type compounds are removed from the atmosphere by reaction with the major oxidants OH, NO_3 and O_3. There have been
44 a number of studies on the rates of reaction of furan type compounds with the dominant daytime oxidant, OH (Lee and Tang,
45 1982; Atkinson et al., 1983; Wine and Thompson, 1984; Bierbach et al., 1992, 1994, 1995; Aschmann et al., 2011; Ausmeel et
46 al., 2017; Whelan et al., 2020). However, there have been fewer studies on the rates of reaction of furan type compounds with
47 the major night-time oxidant, NO_3 (Atkinson et al., 1985; Kind et al., 1996; Cabañas et al., 2004; Colmenar et al., 2012).

48 The nitrate radical, NO_3, is produced in the atmosphere predominantly through the reaction of NO_2 with O_3, and exists in
49 equilibrium with N_2O_5. It has long been known to be an important night-time oxidant (Levy, 1972; Winer et al., 1984). While it
50 is also produced during the daytime, it is rapidly converted back to NO_2 by reaction with NO and by photolysis. However, in
51 environments with low NO, either due to low NOx emissions, or suppression through high O_3 concentrations (e.g. Newland et
52 al., 2021), NO_3 oxidation has been observed to be significant during the day (Hamilton et al., 2021).

53 Here, we present results of a series of relative rate experiments for furan, 2-methylfuran, 2,5-dimethylfuran, furan-2-aldehyde
54 (furfural), 5-methyl-2(3H)-furanone (α-angelicalactone), 2(5H)-furanone (γ-crotonolactone), and pyrrole reaction with the NO_3
55 radical, performed in the 7300 L indoor simulation chamber at CNRS-ICARE, Orléans, France.

2 Experimental

2.1   CSA-Chamber

59 The CNRS-ICARE indoor chamber is a 7300 L indoor simulation chamber used for studying reaction kinetics and mechanisms
60 under atmospheric boundary layer conditions. Further details of the chamber setup and instrumentation are available elsewhere
61 (Zhou et al., 2017). Experiments were performed in the dark at atmospheric pressure (*ca.* 1000 mbar), with the chamber operated
62 at a slight overpressure to compensate for removal of air for sampling, and to prevent ingress of outside air to the chamber. The
63 chamber is in a climate controlled room and the temperature was maintained at 299±2 K.

2.2   Experimental Approach

67 Starting with the chamber filled with clean air, the VOCs of interest (*ca.* 3 ppmv) were added, followed by ~ 1 Torr of the inert
68 gas SF_6 to monitor the chamber dilution rate. The chamber was left for at least thirty minutes prior to the start of the experiment
69 to monitor the dilution rate and losses of the VOCs to the chamber walls. These losses, $(1-8)\times10^{-6}\,s^{-1}$, were always smaller than
70 dilution ($\sim1.2\times10^{-5}\,s^{-1}$). The reaction was then initiated by continually introducing an N_2O_5 sample, held in a trap at ~ 235 K,
71 with air flow of $(2.5-5)$ L/min through it. The chamber was monitored until most of the VOC of interest was consumed, with
72 experiments generally taking $0.5-2$ hours. The experiments were performed under dry conditions (RH ≤ 1.5 %).

Atmospheric
Chemistry
and Physics
Discussions
Open Access
EGU

73 VOC abundance was determined by *in-situ* Fourier Transform Infrared (FTIR) Spectroscopy using a Nicolet 5700 coupled to a

74 White-type multipass cell with a pathlength of 143 m. Each scan was comprised of either 30 or 60 co-additions depending on
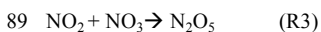
75 the expected rate of loss of the VOCs.

76

77 **2.3   Materials**

78

79 Furan (>99%, Sigma-Aldrich), 2-methylfuran (>98%, TCI), 2,5-dimethylfuran (>98%, TCI), pyrrole (>99%, TCI), α-

80 angelicalactone (>98%, TCI), furfural (>98%, TCI), α-terpinene (90%, Sigma-Aldrich), 2,3-dimethyl-but-2-ene (98%, Sigma-

81 Aldrich), 2-carene (97%, Sigma-Aldrich), camphene (95%, Sigma-Aldrich), α-pinene (98%, Sigma-Aldrich), cyclohexene

82 (≥99%, Sigma-Aldrich), 3-methyl-3-buten-1-ol (97%, Sigma-Aldrich) and γ-crotonolactone (>93%, TCI), were used as supplied

83 without further purification.

84 N_2O_5 was synthesised by reacting NO_2 with excess O_3. First, NO and O_3 were mixed to generate NO_2 (Reaction R1). This NO_2 /

85 O_3 mixture was then flushed into a bulb in which NO_3 and subsequently N_2O_5 were generated through Reactions R2-R3.

86

87 $NO + O_3 \rightarrow NO_2$ (R1)

88 $NO_2 + O_3 \rightarrow NO_3$ (R2)

89 $NO_2 + NO_3 \rightarrow N_2O_5$ (R3)

90

91 N_2O_5 crystals were then collected in a cold trap at 190K. The N_2O_5 sample was purified by trap to trap distillation under a flow

92 of O_2 / O_3. The final sample was stored at 190 K and used within a week.

93

94 **2.4   Analysis**

95

96 VOC concentrations were monitored by FTIR. The furans generally have a number of major absorption bands in the infrared.

97 The main bands used for analysis are shown in Table 1 (bold), as well as other characteristic bands for each compound. Reference

98 spectra of the major bands for each compound taken in the chamber at a resolution of 0.25 cm^{-1} are provided in the Supplement

99 (Figures S1-S7). The ANIR curve fitting software (Ródenas, 2018), which implements a least squares fitting algorithm was used

100 to generate time profiles for each compound based on their reference spectra. Profiles were checked by doing a number of manual

101 subtractions. Example time profiles from an experiment with α-angelicalactone and furan, with cyclohexene as the reference

102 compound, are shown in Figure 1. Relative rate plots from the experiments with furan and 2-methylfuran are shown in Figure 2.

103

104

105

106

107

108

109

110 **Table 1** Maxima of major absorption bands (of Q branches if present) for the compounds used in this study. Bands used
111 predominantly for analysis are shown in bold.

Compound	Main absorption bands / cm^{-1}
Furan	**995**, 744
2-Methylfuran	**792**, 726, 1151, 2965
2,5-Dimethylfuran	**777**, 2938, 2961
Furfural	**756**, 1720
Pyrrole	**724**, 1017, 3531, 718-722
5-Methyl-2(3H)-furanone	**731, 939**, 1100, 1834
2(5H)-furanone	**1098**, 805, 866, 1045, 1812, 2885, 2945

112

113 Relative rate experiments were performed, whereby a compound (or two) with an unknown reaction rate (k_{VOC}) with NO$_3$ was
114 added to the chamber with a reference compound with a known NO$_3$ reaction rate (k_{ref}). A plot of the relative loss of the compound
115 against the reference compound following addition of NO$_3$ (via N$_2$O$_5$ decomposition), accounting for both chamber dilution and
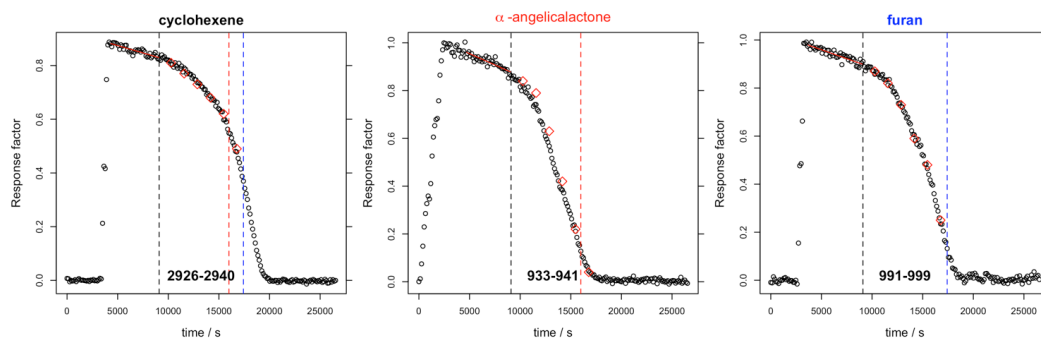116 wall losses (k_d), gives a gradient of k_{VOC}/k_{ref} (Equation E1).

117

118 $$\ln\frac{([VOC]_0)}{([VOC]_t)} - k_d t = \frac{k_{VOC}}{k_{ref}} \ln\frac{[ref]_0}{[ref]_t} - k_d t \qquad (E1)$$

119

120 A number of reference compounds were used for each VOC, chosen so that the reference rate was roughly within a factor of five
121 of the expected unknown rate, and with an attempt to use different references that had both faster and slower NO$_3$ reaction rates
122 than the VOC. Reaction rates of the reference compounds (Table 2) are taken from the Database for the Kinetics of the Gas-
123 Phase Atmospheric Reactions of Organic Compounds v2.1.0 (McGillen et al., 2020), available at data.eurochamp.org/data-
124 access/kin/#/home.

125

126

127 **Figure 1** Concentration-time profiles from experiment with cyclohexene, α-angelicalactone and furan. Black circles are response
128 factors generated by the ANIR curve fitting program relative to the reference spectra. Red diamonds are obtained from manual
129 subtractions. Left black dashed vertical line is the beginning of the region used for the relative rate calculation, the red dashed
130 line is the end of the region used for the calculation of the α-angelicalactone relative rate, the blue line is the end of the region
131 used for the calculation of the furan relative rate. Bold values at the bottom are the absorption bands used for analysis.
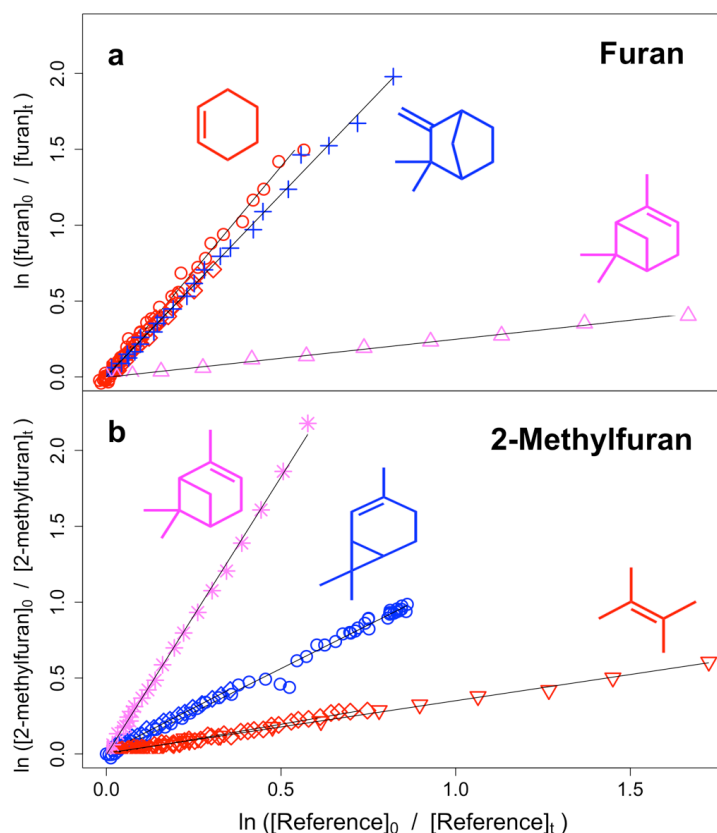
132 **Table 2.** Reference compounds used. Recommended rates and uncertainties from McGillen et al. (2020).

Compound	k / cm^3 molecule^{-1} s^{-1}
2,3-dimethyl-2-butene	$(5.70\pm1.71)\times10^{-11}$
2-carene	$(2.0\pm0.3)\times10^{-11}$
α-pinene	$(6.20\pm1.55)\times10^{-12}$
camphene	$(6.60\pm1.65)\times10^{-13}$
cyclohexene	$(5.60\pm0.84)\times10^{-13}$
3-methyl-3-buten-1-ol	$(2.60\pm0.78)\times10^{-13}$

133

134 It is noted that no OH scavenger was used in these experiments (as is the case for most, if not all, NO$_3$ previous relative rate

135 studies to the authors' knowledge). NO$_3$ reaction with alkenes tends to proceed by electrophilic addition to the double bond

136 followed by addition of O$_2$ to the resulting radical, leading to a nitrooxy peroxy radical (β-ONO$_2$-RO$_2$) (Barnes et al., 1989;

137 Hjorth et al., 1990). It has recently been shown (Novelli et al., 2021) that there is the possibility of OH formation through the

138 reactions of β-ONO$_2$-RO$_2$ with HO$_2$. HO$_2$ could be generated in these experiments from the abstraction of an H atom by O$_2$ from

139 a β-ONO$_2$-RO radical with available H atoms. The initial NO$_3$ reaction with furans is not thought to form β-ONO$_2$-RO$_2$ radicals,

140 with NO$_3$ addition to the C2 carbon followed by O$_2$ addition to the C5 carbon (Berndt et al., 1996), analogous to the OH addition

141 reaction (Bierbach et al., 1995; Mousavipour et al., 2009; Yuan et al., 2017; Whelan et al., 2020). However, some of the reference

142 compounds used in the experiments will form such radicals. For example, the reaction of HO$_2$ with the β-ONO$_2$-RO$_2$ radicals

143 formed from α-pinene + NO$_3$ has been reported to have an OH yield of up to 70 % (Kurtén et al., 2017). A box model run was

144 performed to test the impact of this chemistry in this study. The α-pinene scheme from the MCMv3.3.1 (Jenkin et al., 1997;

145 mcm.york.ac.uk) was incorporated into the box model AtChem (Sommariva et al., 2020), and an OH yield of 0.5 was assigned

146 to the reaction of HO$_2$ with the initial β-ONO$_2$-RO$_2$ radicals formed from the α-pinene+NO$_3$ reaction. The model was initiated

147 with 2-methylfuran and α-pinene concentrations of 3 ppmv, representative of the experiments performed here. NO$_3$

148 concentrations were constrained to give a lifetime of ~ 1 hour for the VOCs, typical of the experiments. OH reaction was found

149 to account for less than 1 % of the removal of 2-methylfuran or α-pinene through the model run. Consequently, it can be assumed

150 that OH chemistry is a negligible interference in these experiments.

151

Figure 2. Relative rate plots for: **a.** furan relative to cyclohexene (red), camphene (blue), and α-pinene (pink); **b.** 2-methylfuran relative to 2-carene (blue), 2,3-dimethyl-2-butene (red), and α-pinene (pink). Different shapes are used for different experiments with the same reference compound.

3 Results and Discussion

The $k(NO_3)$ rate coefficients determined with each reference compound are given in Table 3 and Figure 3. A recommendation of an updated rate coefficient for α-terpinene+NO$_3$ is also given in Table 3. Overall recommended values for the rate coefficient for each compound are calculated by taking the mean (weighted by the reported uncertainty of the reference) of the rate coefficient derived from each experiment with each reference compound, including using the recommended values for the other furans and for α-terpinene presented in Table 3. Uncertainties for the relative rates in Table S1 are assumed to be < 10 % and to be dominated by statistical errors in fitting to the absorption bands. Uncertainties for the rate coefficients reported in Table 3 are dominated by the assumed uncertainties in $k(NO_3)$ of the reference compounds. For most of the references, the uncertainties are 20 – 30 %, taken from the recommendations of McGillen et al. (2020). For 2,3-dimethyl-2-butene, the recommended uncertainty

Atmospheric
Chemistry
and Physics
Discussions

Open Access

EGU

165   in McGillen et al. (2020) is 150 %, but based on the fact that the rate coefficients derived using 2,3-dimethyl-2-butene for 2-

166   methylfuran, 2,5-dimethylfuran and pyrrole agree very well with those using other references with much smaller uncertainties,

167   a conservative estimate of 30 % is used here. It is noted that for all compounds, the rate coefficients derived with different

168   references agree very well, to within 10%, with the exception of α-terpinene, which is discussed further below. The

169   experimentally determined $k(NO_3)$ rates of the furans relative to each other are in good agreement (to within 6%) with those

170   calculated using the weighted means shown in Table 3 (Table S2). This gives further confidence in the $k(NO_3)$ values used for

171   the reference compounds.

172

173   The rate coefficient derived for furan, agrees well with the value previously reported by Atkinson et al. (1985) from a chamber

174   relative rate experiment. However, there is significant differences between the values reported here for furan, 2-methylfuran and

175   2,5-dimethylfuran, and those reported by Kind et al. (1996) from relative rate experiments in a flow reactor. While the value

176   reported for 2-methylfuran agrees within the uncertainties between the two studies, the values for furan and 2,5-dimethylfuran

177   are ~ 50 % and 100 % greater respectively. It is unclear what is behind this observed disparity; the good agreement between the

178   two studies for the 2-methylfuran rate coefficient suggests that there is not a systematic difference between the experimental

179   setups. For pyrrole, the rate coefficient determined here is about 50% faster than the value reported by Atkinson et al. (1985)

180   from a chamber relative rate experiment using N_2O_5 thermal decomposition. Cabañas et al. (2004) reported an upper limit of

181   $<1.8\times10^{-10}$ cm^3 molecule^{-1} s^{-1} (298K) using an absolute technique of fast flow discharge.

182   For 2-furanaldehyde (furfural) + NO_3, the rate coefficient recommended here is an order of magnitude slower than the only

183   previously reported values (Colmenar et al., 2012), derived from small chamber relative rate experiments with 2-methyl-2-butene

184   and α-pinene as references. The rate coefficient from Colmenar et al. (2012) is very similar to the reported rate coefficient for

185   furan+NO_3. This is surprising, since the presence of a formyl group attached to a double bond is expected to be strongly

186   deactivating with respect to addition to that bond, due to the electron withdrawing mesomeric effect of the –C(O)H group

187   (Kerdouci et al., 2014). This has also been observed for other electrophilic addition reactions, such as those with OH and O_3

188   (Kwok and Atkinson, 1995; McGillen et al, 2011; Jenkin et al., 2020). And while there is the possibility of H abstraction from

189   the formyl group, which would increase the overall rate coefficient, such reactions are typically of the order of 10^{-14} cm^{3}s^{-1}

190   (Kerdouci et al., 2014), and hence would not be expected to compensate for the reduced rate of the addition reaction.

191   For 5-methyl-(3H)-furan-2-one (α-angelica lactone) + NO_3 this is the first reported rate coefficient. For (5H)-furan-2-one (γ-

192   crotonolactone), relative rate experiments with several reference compounds were attempted, with the slowest reacting of these

193   being cyclohexane (k_{NO3} = 1.4×10^{-16} cm^3 molecule^{-1} s^{-1}). Roughly 10 % of the cyclohexane was removed in this experiment

194   (accounting for loss by dilution), with no appreciable loss of γ-crotonolactone. We can therefore deduce that k(γ-

195   crotonolactone+NO_3) << 1.4×10^{-16} cm^3 molecule^{-1} s^{-1}. Again, this is the first time a NO_3 reaction rate has been measured for this

196   compound. A comparison of the two furanones shows that 5-methyl-(3H)-furan-2-one reacts more than four orders of magnitude

197   faster than (5H)-furan-2-one. This can be explained in part by the presence of a methyl group, which is seen to increase the rate

198   by roughly an order of magnitude from e.g. furan to 2-methylfuran to 2,5-dimethylfuran. Berndt et al. (1997) derived an NO_3

199   reaction rate of 1.76×10^{-13} cm^3 molecule^{-1} s^{-1} for (3H)-furan-2-one. However, the majority of the difference must be explained by

200   the structure of the two compounds, namely the conjugated nature of the C=C and C=O bonds in (5H)-furan-2-one. The carbonyl

201   group removes electron density from the C=C bond greatly reducing the rate coefficient. A similar relationship is seen for
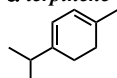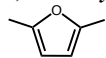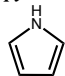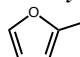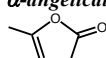
Atmospheric
Chemistry
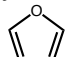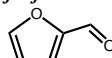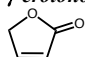and Physics
Discussions
Open Access

202 analogous acyclic compounds e.g. the NO_3 rate coefficient of the conjugated ester methyl acrylate is almost two orders of

203 magnitude greater than that of the non-conjugated isomer vinyl acetate.
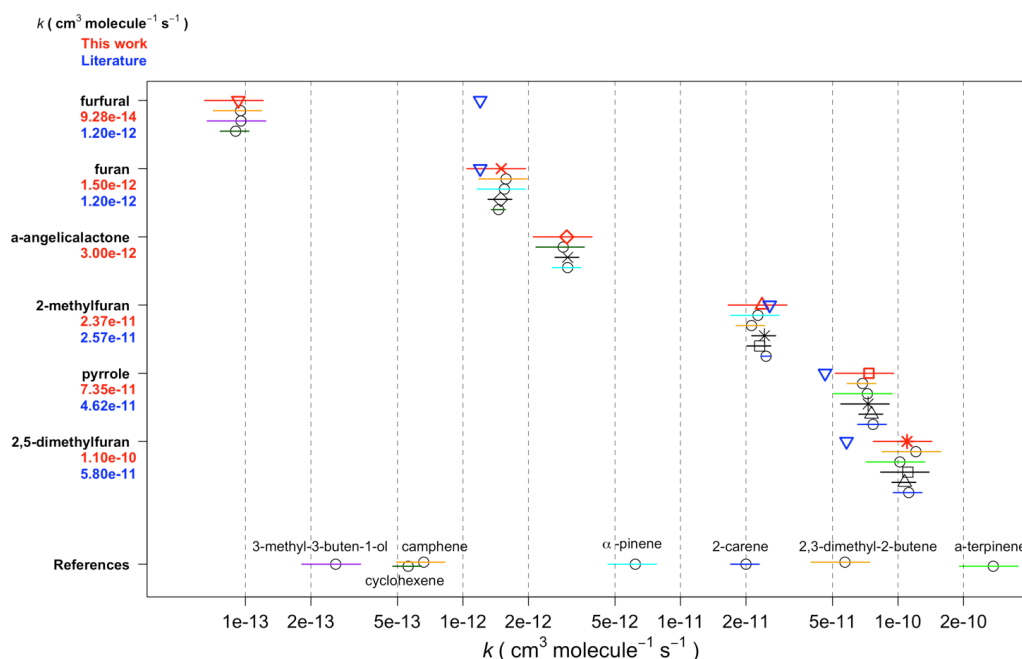
204

205

206 **Table 3.** NO_3 reaction rate coefficients derived for each experiment and recommended value based on the weighted mean.

Compound	Reference (repeats)	$k(NO_3)$ / cm³ molecule⁻¹ s⁻¹	Weighted mean $k(NO_3)$ / cm³ molecule⁻¹ s⁻¹
α-terpinene	2,5-dimethylfuran (1)	2.92×10^{-10}	$\mathbf{2.74\pm0.81\times10^{-10}}$
	2,3-dimethyl-2-butene (1)	2.50×10^{-10}	
	pyrrole (1)	2.69×10^{-10}	
2,5-dimethylfuran	2-carene (1)	1.12×10^{-10}	$\mathbf{1.10\pm0.33\times10^{-10}}$
	2,3-dimethyl-2-butene (1)	1.21×10^{-10}	
	a-terpinene (1)	1.01×10^{-10}	
	pyrrole (1)	1.10×10^{-10}	
	2-methylfuran (2)	1.07×10^{-10}	
pyrrole	2-carene (1)	7.68×10^{-11}	$\mathbf{7.35\pm2.06\times10^{-11}}$
	2,3-dimethyl-2-butene (2)	6.87×10^{-11}	
	a-terpinene (1)	7.15×10^{-11}	
	2,5-dimethylfuran (1)	7.22×10^{-11}	
	2-methylfuran (2)	7.52×10^{-11}	
2-methylfuran	2-carene (3)	2.47×10^{-11}	$\mathbf{2.37\pm0.55\times10^{-11}}$
	2,3-dimethyl-2-butene (2)	2.12×10^{-11}	
	α-pinene (1)	2.27×10^{-11}	
	pyrrole (2)	2.28×10^{-11}	
	2,5-dimethylfuran (2)	2.41×10^{-11}	
α-angelicalactone	α-pinene	3.03×10^{-12}	$\mathbf{3.00\pm0.45\times10^{-12}}$
	cyclohexene	2.89×10^{-12}	
	furan (2)	3.05×10^{-12}	
furan	cyclohexene	1.46×10^{-12}	$\mathbf{1.50\pm0.23\times10^{-12}}$
	α-pinene	1.55×10^{-12}	
	camphene	1.58×10^{-12}	
	α-angelicalactone (2)	1.49×10^{-12}	
furfural	cyclohexene (1)	9.02×10^{-14}	$\mathbf{9.28\pm2.30\times10^{-14}}$
	3-methyl-3-buten-1-ol (1)	9.54×10^{-14}	
	camphene (1)	9.50×10^{-14}	
γ-crotonolactone	cyclohexane	$< 1.4\times10^{-16}$	$\mathbf{< 1.4\times10^{-16}}$

207

208

209

Figure 3 The reaction rate coefficients derived for the six compounds in this work (excluding α-terpinene). Red triangles (and red text, left axis) represent the weighted mean of all experiments in this work, blue inverted triangles (and blue text, left axis) are the recommended values from McGillen et al. (2020). Horizontal lines represent uncertainty in rate coefficient, colours (shapes if other furans) represent which reference was used.

214

215 α-terpinene was used as a reference compound in two experiments. However, the rate coefficients derived for 2,5-dimethylfuran and pyrrole are significantly smaller using α-terpinene compared to other reference compounds. In addition, its reaction rate relative to 2,3-dimethyl-2-butene is larger than expected based on the recommended rate coefficient of $(1.80\pm1.44)\times10^{-10}$ cm^3 $molecule^{-1}s^{-1}$ (McGillen et al., 2020). The reaction with α-terpinene is one of the largest known VOC+NO$_3$ rate coefficients, and hence it is a useful reference and important to know the rate with a good degree of certainty. We derive a rate coefficient relative to 2,5-dimethylfuran of 2.68, to pyrrole of 3.79 and to 2,3-dimethyl-2-butene of 4.39. Using the recommended values given in Table 3 for 2,5-dimethylfuran and pyrrole, and the recommended value for 2,3-dimethyl-2-butene in Table 2, gives an average NO$_3$ reaction rate for α-terpinene of $(2.70\pm0.81)\times10^{-10}$ cm^3 $molecule^{-1}s^{-1}$. This is considerably faster than a recent absolute rate measurement of $(1.2\pm0.3)\times10^{-10}$ cm^3 $molecule^{-1}s^{-1}$ (Fouqueau et al., 2020), and previous relative rate determinations of $(1.6\pm0.6)\times10^{-10}$ cm^3 $molecule^{-1}s^{-1}$ (Atkinson et al., 1985) and $(0.9\pm0.4)\times10^{-10}$ (Berndt et al., 1996) using TME as a reference.

225

226

227 **Table 4.** Recommended NO_3 rate coefficients from this work compared to those reported in the literature.

Compound	Rate / cm^3 $molecule^{-1}$ s^{-1}	Reference	Technique	NO_3 source
α-terpinene	**(2.74±0.81)×10⁻¹⁰**	**This work**		
	(1.6±0.6)×10⁻¹⁰	Atkinson et al. (1985)	Relative (2,3-dimethyl-2-butene)	
	(0.9±0.4)×10⁻¹⁰	Berndt et al. (1996)	Relative (2,3-dimethyl-2-butene)	
	(1.2±0.3)×10⁻¹⁰	Fouqueau et al. (2020)		
2,5-dimethylfuran	**(1.10±0.33)×10⁻¹⁰**	**This work**		
	(5.78±0.34)×10⁻¹¹	Kind et al. (2006)	Flow reactor: relative (*trans*-2-butene)	N_2O_5
pyrrole	**(7.35±2.06)×10⁻¹¹**	**This work**		
	(4.6±1.1)×10⁻¹¹	Atkinson et al. (1985)	Chamber: relative (2-methyl-2-butene)	N_2O_5
	< 1×10⁻¹⁰	Cabañas et al. (2004)	Flow reactor: absolute (LIF detection of NO_3)	HNO_3+F
2-methylfuran	**(2.37±0.55)×10⁻¹¹**	**This work**		
	(2.57±0.17)×10⁻¹¹	Kind et al. (2006)	Flow reactor: relative (*trans*-2-butene)	N_2O_5
α-angelicalactone	**(3.00±0.45)×10⁻¹²**	**This work**		
furan	**(1.50±0.23)×10⁻¹²**	**This work**		
	(1.5±0.2)×10⁻¹² [a]	Atkinson et al. (1985)	Chamber: relative (*trans*-2-butene)	N_2O_5
	(0.998±0.062)×10⁻¹²	Kind et al. (2006)	Flow reactor: relative (*trans*-2-butene)	N_2O_5
	(1.36±0.8)×10⁻¹²	Cabañas et al. (2004)	Flow reactor: absolute (LIF detection of NO_3)	HNO_3+F
furfural	**(9.28±2.30)×10⁻¹⁴**	**This work**		
	(1.17±0.15)×10⁻¹²	Colmenar et al. (2012)	Small chamber: relative (2-methyl-2-butene)	N_2O_5
	(1.36±0.38)×10⁻¹²	Colmenar et al. (2012)	Small chamber: relative (α-pinene)	N_2O_5
γ-crotonolactone	**< 1.4×10⁻¹⁶**	**This work**		

228 [a] corrected for change to recommended rate for reference (trans-2-butene)

229

230 **Atmospheric implications**

231

232 The atmospheric lifetimes of the compounds, based on the rate coefficients reported herein, are given in Table 5. These assume

233 concentrations of OH = $5×10^6$ molecules cm^{-3} (typical daily peak summertime concentrations $1.5×10^6$ – $1.5×10^7$ molecules cm^{-3}

234 ³ (Stone et al., 2012)), night-time NO_3 = $2×10^8$ molecules cm^{-3} (typical night-time concentrations $1×10^8$ – >$1×10^9$ cm^{-3} (Brown

235 and Stutz (2012)) daytime NO_3 = $1×10^7$ molecules cm^{-3} (limited daytime measurements suggest concentrations ~ 0.5 – >1 pptv

236 ($2.5×10^7$ molecules cm^{-3}) (Brown and Stutz (2012)), and O_3 = 40 ppbv (background O_3 concentration ~ 40 ppb (Parrish et al.,

237 2014)). From these values it is clear that the alkyl substituted furans and pyrrole have very short lifetimes both during the day,

238 when the dominant daytime sink is likely to be reaction with OH, and at night, when the dominant sink will be reaction with

239 NO_3. O_3 may contribute somewhat to the removal of these compounds both during the day and night, particularly for 2,5-

240 dimethylfuran. As $k(NO_3)$ approaches the same order of magnitude as $k(OH)$, e.g. for 2-methylfuran, 2,5-dimethylfuran and

241 pyrrole, the NO_3 reaction is likely to be competitive with the OH reaction even during the day in low NOx environments, with

242 daytime NO_3 concentrations reported to be ~ 1 ppt (2.5×10^7 molecules cm^{-3}) (Brown and Stutz, 2012). The relatively large rate

243 coefficient reported here for 5-methyl-2(3H)-furanone, suggests that NO_3 reaction will be an important sink for unsaturated non-

244 conjugated cyclic esters. On the other hand, the very slow rate of the 2(5H)-furanone+NO_3 reaction suggests that this will not be

245 an important atmospheric sink. 2(5H)-furanone has also been shown to have a very slow reaction with O_3 (lifetime > 100 years,

246 Ausmeel et al., 2017), whereas for reaction with OH, the lifetime is much shorter, and this will be the predominant gas-phase

247 sink for 2(5H)-furanone. Such a slow NO_3 reaction might be expected to extend to all 2-furanones with a conjugated structure,

248 e.g. hydroxyfuranones – major products of OH oxidation of methyl substituted furans (Aschmann et al., 2014), such that the

249 nitrate reaction may be unimportant in the atmosphere for these structures. Although substitution at the double bond is likely to

250 increase the rate coefficient somewhat, as observed for OH and O_3 reactions with the methyl-substituted form of 2(5H)-furanone

251 (Ausmeel et al., 2017).

252 One of the major sources of furan type compounds to the atmosphere is wildfires. Wildfire plumes can be regions of high NO_3

253 even during the day due to suppressed photolysis rates in optically thick plumes (Decker et al, 2021). NO_3 oxidation of furans

254 may be even more important in such plumes than in the background atmosphere. Such plumes can extend over hundreds of

255 kilometres and hence affect air quality on a local and regional scale (e.g. Andreae et al., 1988; Brocchi et al., 2018; Johnson et

256 al., 2021). Domestic wood burning is an increasing trend in northern European cities (Chafe et al., 2015). Burning will generally

257 be in the winter during which, with short daylight hours and peak daytime OH often an order of magnitude lower than during

258 the summer, the reaction with NO_3 is likely to be the dominant fate of furan type compounds in such emissions, contributing

259 significantly to organic aerosol in urban areas (Kodros et al., 2020).

260 Berndt et al. (1996) identified the major first generation products of furan+NO_3 to be the unsaturated dicarbonyl, butenedial, and

261 2(3H)-furanone, with the NO_3 recycled back to NO_2. However, Tapia et al. (2011), and Joo et al. (2019) found that the major

262 products of the 3-methylfuran+NO_3 reaction predominantly retain the NO_3 functionality. In this case, furan+NO_3 oxidation

263 chemistry may be a significant sink for NOx, sequestering it in nitrate species, which might release it far from source on further

264 gas-phase oxidation, or, due to their low volatility, be taken up into aerosol (Joo et al. 2019).

265

266

267

268

269

270

271

272

273

274

275

276 **Table 5.** Atmospheric gas-phase lifetimes of the compounds reported herein based on typical mid-day OH concentrations of

277 5×10^6 molecules cm^{-3}, night-time NO$_3$ concentrations of 2×10^8 molecules cm^{-3}, day-time NO$_3$ concentrations of 1×10^7 molecules

278 cm^{-3}, and background O$_3$ concentrations of 40 ppbv (1×10^{12} molecules cm^{-3}).

Compound	$\tau_{NO3\,(night)}$	$\tau_{NO3\,(day)}$	$\tau_{OH\,(day)}$	τ_{O3}	$\tau_{total\,(day)}$
2,5-dimethylfuran	0.76 min	15 min	26 min [a]	40 min [b]	8 min
2-methylfuran	3.5 min	70 min	48 min [a]	-	28 min
furan	56 min	19 hours	83 min [a]	116 hours [c]	77 min
pyrrole	1.1 min	23 min	28 min [d]	18 hours [d]	13 mins
furfural	15 hours	12 days	95 min [e]	-	94 min
5-methyl-2(3H)-furanone	28 min	9.3 hours	48 min [f]	3.5 hours [g]	37 mins
2(5H)-furanone	> 1.1 year	> 22 years	14 hours [h]	173 years	14 hours

279 [a] Matsumoto (2011); [b] Dillon et al. (2012); [c] Atkinson et al. (1983); [d] Atkinson et al. (1984); [e] Bierbach et al. (1995); [f] Bierbach

280 et al. (1994); [g] estimated (Bierbach et al., 1994); [h] Ausmeel et al. (2017)

281

282 **4 Conclusions**

283 Rate coefficients are recommended for reaction of seven furan type VOCs with NO$_3$ at 298 K and 760 Torr, based on a series of

284 relative rate experiments. These new recommendations highlight the importance of NO$_3$ chemistry to the removal of furans, and

285 other similar VOCs, under atmospheric conditions. The measured rate coefficients suggest that for the three furans reported here,

286 as well as for pyrrole and 5-methyl-2(3H)-furanone, reaction with NO$_3$ is likely to be their dominant night-time sink. For the

287 alkyl furans and pyrrole, reaction with NO$_3$ may also be a significant sink during the daytime. In addition to the rates for the

288 furan type compounds, an updated recommendation is provided for $k(\alpha$-terpinene+NO$_3$), a reaction of particular importance as

289 one of the fastest known VOC+NO$_3$ reaction rate coefficients. This work also extends the existing database of VOC+NO$_3$

290 reactions, providing valuable reference values for future work.

291

292

293 *Data availability.* All relevant data and supporting information have been provided in the Supplement.

294

Atmospheric
Chemistry
and Physics
Discussions

295 *Author contributions.* MJN performed the experiments with the technical support of YR and MRM and performed the data
296 treatment and interpretation. MJN wrote the paper. All coauthors revised the content of the original manuscript and approved
297 the final version of the paper.
298
299 *Competing interests.*
300 The authors declare that they have no conflict of interest.
301
302 *Special issue statement.* This article is part of the special issue "Simulation chambers as tools in atmospheric research
303 (AMT/ACP/GMD inter-journal SI)". It is not associated with a conference.
304

313 **References**

314 Ahern, A. T., Robinson, E. S., Tkacik, D. S., Saleh, R., Hatch, L. E., Barsanti, K. C., Stockwell, C. E., Yokelson, R. J., Presto,
315 A. A., Robinson, A. L., Sullivan, R. C., and Donahue, N. M.: Production of Secondary Organic Aerosol During Aging of Biomass
316 Burning Smoke From Fresh Fuels and Its Relationship to VOC Precursors, J. Geophys. Res.-Atmos., 124, 3583–3606, 2019.
317
318 Akherati, A., He, Y., Coggon, M. M., Koss, A. R., Hodshire, A. L., Sekimoto, K., Warneke, C., de Gouw, J., Yee, L., Seinfeld,
319 J. H., Onasch, T. B., Herndon, S. C., Knighton, W. B., Cappa, C. D., Kleeman, M. J., Lim, C. Y., Kroll, J. H., Pierce, J. R., and
320 Jathar, S. H.: Oxygenated Aromatic Compounds are Important Precursors of Secondary Organic Aerosol in Biomass Burning
321 Emissions, Environ. Sci. Technol., 54, 8568–8579, https://doi.org/10.1021/acs.est.0c01345, 2020.
322
323 Andreae, M. O., Browell, E. V., Garstang, M,. Gregory, G. L., Harriss, R. C., Hill, G. F., Jacob, D. J., Pereira, C., Sachse, G. W.,
324 Setzer, A. W., Silva Dias, P. L., Talbot, R. W., Torres, A. L., and Wofsy, S. C.: Biomass-burning emissions and associated haze
325 layers over Amazonia, J. Geophys. Res.-Atmos, 93, 1509-1527, 1988.
326
327 Andreae, M. O.: Emission of trace gases and aerosols from biomass burning – an updated assessment, Atmos. Chem. Phys., 19,
328 8523–8546, https://doi.org/10.5194/acp-19-8523-2019, 2019.

13

329

330 Aschmann, S. M., Nishino, N., Arey J., and Atkinson, R.: Products of the OH radical-initiated reactions of furan, 2- and 3-
331 methylfuran, and 2,3- and 2,5-dimethylfuran in the presence of NO, J. Phys. Chem. A, 118, 457-466, 2014.
332

333 Atkinson, R., Aschmann, S. M., and Carter, W. P. L.: Kinetics of the reactions of O3 and OH radicals with furan and thiophene
334 at 298 +/- 2 K, Int. J. Chem. Kinet., 15, 51-61, 1983.
335

336 Atkinson, R., Aschmann, S. M., Winer, A. M., and Carter, W. P. L.: Rate Constants for the Gas Phase Reactions of OH Radicals
337 and O_3 with Pyrrole at 295 +/- 1 K and Atmospheric Pressure, Atmos. Environ., 18, 2105-2107, 1984.
338

339 Atkinson, R., Aschmann, S. M., Winer, A. M., and Carter, W. P. L.: Rate Constants for the Gas Phase Reactions of NO_3 Radicals
340 with Furan, Thiophene and Pyrrole at 295 +/- 1 K and Atmospheric Pressure, Environ. Sci. Technol., 19, 87-90, 1985.
341

342 Ausmeel, S., Andersen, C., Nielsen, O. J., Østerstrøm, F. F., Johnson, M. S., and Nilsson, E. J. K.: Reactions of Three Lactones
343 with Cl, OD, and O_3: Atmospheric Impact and Trends in Furan Reactivity, J. Phys. Chem. A, 121, 4123-4131, 2017.
344

345 Barnes, I., Bastian, V., Becker, K. H., and Tong, Z.: Kinetics and products of the reactions of nitrate radical with monoalkenes,
346 dialkenes, and monoterpenes, J. Phys. Chem., 94, 2413–2419, 1990.
347

348 Berndt, T., Böge, O., and Rolle, W.: Products of the Gas-Phase Reactions of NO_3 Radicals with Furan and Tetramethylfuran,
349 Environ. Sci. Technol., 31, 1157–1162, 1997.
350

351 Bierbach, A., Barnes, I., Becker, K. H., and Wiesen, E.: Atmospheric Chemistry of Unsaturated Carbonyls: Butenedial, 4-Oxo-
352 2-pentenal, 3-Hexene-2,5-dione, Maleic Anhydride, 3H-Furan-2-one, and 5-Methyl-3H-furan-2-one, Environ. Sci. Technol., 28,
353 715-729, 1994.
354

355 Bierbach, A., Barnes, I., and Becker, K. H.: Product and kinetic study of the OH-initiated gas-phase oxidation of furan, 2-
356 methylfuran and furanaldehydes at ≈ 300 K, Atmos. Environ., 29, 2651–2660, 1995.
357

358 Binder, J. B., and Raines, R. T.: Simple Chemical Transformation of Lignocellulosic Biomass into Furans for Fuels and
359 Chemicals. J. Am. Chem. Soc., 131, 1979−1985, 2009.
360

361 Bloss, C., Wagner, V., Jenkin, M. E., Volkamer, R., Bloss, W. J., Lee, J. D., Heard, D. E., Wirtz, K., Martin-Reviejo, M., Rea,
362 G., Wenger, J. C., and Pilling, M. J.: Development of a detailed chemical mechanism (MCMv3.1) for the atmospheric oxidation
363 of aromatic hydrocarbons, Atmos. Chem. Phys., 5, 641–664, https://doi.org/10.5194/acp-5-641-2005, 2005.
364

365 Brocchi, V., Krysztofiak, G., Catoire, V., Guth, J., Marécal, V., Zbinden, R., El Amraoui, L., Dulac, F., and Ricaud, P.:
366 Intercontinental transport of biomass burning pollutants over the Mediterranean Basin during the summer 2014 ChArMEx-
367 GLAM airborne campaign, Atmos. Chem. Phys., 18, pp. 6887-6906, 2018.
368

369 Brown, S., and Stutz, J.: Nighttime radical observations and chemistry, Chem. Soc. Rev., 41, 6405-6447, 2012.
370

371 Cabañas, B., Baeza, M. T., Salgado, S., Martín, P., Taccone, R., and Martínez, E.: Oxidation of heterocycles in the atmosphere:
372 Kinetic study of their reactions with NO_3 radical, J. Phys. Chem. A, 108, 10818-10823, 2004.
373
374 Chafe, Z., Brauer, M., Héroux, M. –E., Klimont, Z., Lanki, T., Salonen, R. O., and Smith, K. R.: Residential heating with wood
375 and coal: health impacts and policy options in Europe and North America, WHO Regional Office for
376 Europe. https://apps.who.int/iris/handle/10665/153671, 2015.
377
378 Coggon, M. M., Lim, C. Y., Koss, A. R., Sekimoto, K., Yuan, B., Gilman, J. B., Hagan, D. H., Selimovic, V., Zarzana, K. J.,
379 Brown, S. S., M Roberts, J., Müller, M., Yokelson, R., Wisthaler, A., Krechmer, J. E., Jimenez, J. L., Cappa, C., Kroll, J. H., De
380 Gouw, J. and Warneke, C.: OH chemistry of non-methane organic gases (NMOGs) emitted from laboratory and ambient biomass
381 burning smoke: Evaluating the influence of furans and oxygenated aromatics on ozone and secondary NMOG formation, Atmos.
382 Chem. Phys., 19, 14875–14899, doi:10.5194/acp-19-14875-2019, 2019.
383
384 Colmenar, I., Cabañas, B., Martínez, E., Salgado, M. S., and Martín, P.: Atmospheric fate of a series of furanaldehydes by their
385 NO_3 reactions, Atmos. Environ., 54, 177-184, 2012.
386
387 Decker, Z. C. J., Zarzana, K. J., Coggon, M., Min, K.-E., Pollack, I., Ryerson, T. B., Peischl, J., Edwards, P., Dubé, W. P.,
388 Markovic, M. Z., Roberts, J. M., Veres, P. R., Graus, M., Warneke, C., de Gouw, J., Hatch, L. E., Barsanti, K. C. and Brown, S.
389 S.: Nighttime Chemical Transformation in Biomass Burning Plumes: A Box Model Analysis Initialized with Aircraft
390 Observations, Environ. Sci. Technol., 53, 2529–2538, doi:10.1021/acs.est.8b05359, 2019.
391
392 Dillon, T. J., Tucceri, M. E., Dulitz, K., Horowitz, A., Vereecken, L., and Crowley, J.: Reaction of Hydroxyl Radicals with
393 C4H5N (Pyrrole): Temperature and Pressure Dependent Rate Coefficients, J. Phys. Chem. A, 116, 6051-6058, 2012.
394
395 Fouqueau, A., Cirtog, M., Cazaunau, M., Pangui, E., Doussin J. -F., and Picquet-Varrault, B.: A comparative and experimental
396 study of the reactivity with nitrate radical of two terpenes: α-terpinene and γ-terpinene, Atmos. Chem. Phys., 20, 15167-15189,
397 2020.
398
399 Harvey B. J.: Human-caused climate change is now a key driver of forest fire activity in the western United States, Proc. Natl.
400 Acad. Sci., 113, 11649-11650, 2016.
401
402 Hartikainen, A., Yli-Pirilä, P., Tiitta, P., Leskinen, A., Kortelainen, M., Orasche, J., Schnelle-Kreis, J., Lehtinen, K.,
403 Zimmermann, R., Jokiniemi, J., and Sippula, O.: Volatile Organic Compounds from Logwood Combustion: Emissions and
404 Transformation under Dark and Photochemical Aging Conditions in a Smog Chamber, Environ. Sci. Technol., 52, 4979-4988,
405 2018.
406
407 Hatch, L. E., Luo, W., Pankow, J. F., Yokelson, R. J., Stockwell, C. E., and Barsanti, K. C.: Identification and quantification of
408 gaseous organic compounds emitted from biomass burning using two-dimensional gas chromatography–time-of-flight mass
409 spectrometry, Atmos. Chem. Phys., 15, 1865–1899, https://doi.org/10.5194/acp-15-1865-2015, 2015.
410

Atmospheric
Chemistry
and Physics
Discussions

411 Hatch, L. E., Yokelson, R. J., Stockwell, C. E., Veres, P. R., Simpson, I. J., Blake, D. R., Orlando, J. J., and Barsanti, K. C.:
412 Multi-instrument comparison and compilation of non-methane organic gas emissions from biomass burning and implications for
413 smoke-derived secondary organic aerosol precursors, Atmos. Chem. Phys., 17, 1471–1489, 2017.
414
415 Hjorth, J., Lohse, C., Nielsen, C. J., Skov, H., and Restelli, G.: Products and mechanism of the gas-phase reaction between
416 NO_3 and a series of alkenes, J. Phys. Chem., 94, 7494–7500, 1990.
417
418 Jenkin, M. E., Saunders, S. M., and Pilling, M. J.: The tropospheric degradation of volatile organic compounds: a protocol for
419 mechanism development, Atmos. Environ., 31, 81–104, https://doi.org/10.1016/S1352-2310(96)00105-7, 1997 (data available
420 at: http://mcm.york.ac.uk, last access: 12 August 2021).
421
422 Jenkin, M. E., Valorso, R., Aumont, B., Newland, M. J., and Rickard, A. R.: Estimation of rate coefficients for the reactions of
423 O_3 with unsaturated organic compounds for use in automated mechanism construction, Atmos. Chem. Phys., 20, 12921–12937,
424 https://doi.org/10.5194/acp-20-12921-2020, 2020.
425
426 Johnson, M. S., Strawbridge, K., Knowland, K. E., Keller, C., and Travis, M.: Long-range transport of Siberian biomass burning
427 emissions to North America during FIREX-AQ, Atmos. Environ., 252, 118241, 2021
428
429 Jolly, W. M., Cochrane, M. A., Freeborn, P. H., Holden, Z. A., Brown, T. J., Williamson, G. J., and Bowman, D. M. J. S.:
430 Climate-induced variations in global wildfire danger from 1979 to 2013, Nat. Commun., 6, 7537, 2015.
431
432 Kerdouci, J., Picquet-Varrault, B., and Doussin, J. –F.: Structure activity relationship for the gas-phase reactions of NO_3 radical
433 with organic compounds: Update and extension to aldehydes, Atmos. Environ., 84, 363-372, 2014.
434
435 Kind, I., Berndt, T., Böge, O., and Rolle, W.: Gas-phase rate constants for the reaction of NO_3 radicals with furan and methyl-
436 substituted furans, Chem. Phys. Lett., 256, 679-683, 1996.
437
438 Kodros, J., Papanastasiou, D., Paglione, M., Masiol, M. and Squizzato, S.: Rapid dark aging of biomass burning as an overlooked
439 source of oxidized organic aerosol, 117, 33028-33033, 2020.
440
441 Koss, A. R., Sekimoto, K., Gilman, J. B., Selimovic, V., Coggon, M. M., Zarzana, K. J., Yuan, B., Lerner, B. M., Brown, S. S.,
442 Jimenez, J. L., Krechmer, J., Roberts, J. M., Warneke, C., Yokelson, R. J., and de Gouw, J.: Non-methane organic gas emissions
443 from biomass burning: identification, quantification, and emission factors from PTR-ToF during the FIREX 2016 laboratory
444 experiment, Atmos. Chem. Phys., 18, 3299–3319, https://doi.org/10.5194/acp-18-3299-2018, 2018.
445
446 Krikken, F., Lehner, F., Haustein, K., Drobyshev, I., and van Oldenborgh, G. J.: Attribution of the role of climate change in the
447 forest fires in Sweden 2018, Nat. Hazards Earth Syst. Sci., 21, 2169–2179, https://doi.org/10.5194/nhess-21-2169-2021, 2021.
448
449 Kurtén, T., Møller, K. H., Nguyen, T. B., Schwantes, R. H., Misztal, P. K., Su, L., Wennberg, P. O., Fry J. L., and Kjaergaard,
450 H. G.: Alkoxy Radical Bond Scissions Explain the Anomalously Low Secondary Organic Aerosol and Organonitrate Yields
451 From alpha-Pinene + NO_3, J. Phys. Chem. Lett., 8, 2826–2834, 2017.
452

453   Kwok, E. S. C., and Atkinson, R.: Estimation of hydroxyl radical reaction rate constants for gas-phase organic compounds using
454   a structure-reactivity relationship: An update, Atmos. Environ., 29, 1685-1695, 10.1016/1352-2310(95)00069-b, 1995.
455

456   Lohmander, P.: Forest fire expansion under global warming conditions: Multivariate estimation, function properties, and
457   predictions for 29 countries, Central Asian Journal of Environmental Science and Technology Innovation, 5, 262-276, 2020.
458

459   Matsumoto, J.: Kinetics of the reactions of ozone with 2,5-dimethylfuran and its atmospheric implications, Chem. Lett., 40, 582-
460   583, 2011.
461

462   McGillen, M. R., Archibald, A. T., Carey, T., Leather, K. E., Shallcross, D. E., Wenger, J. C., and Percival, C. J.: Structure-
463   activity relationship (SAR) for the prediction of gas-phase ozonolysis rate coefficients: an extension towards heteroatomic
464   unsaturated species, Phys. Chem. Chem. Phys., 13, 2842-2849, 2011.
465

466   McGillen, M. R., Carter, W. P. L., Mellouki, A., Orlando, J. J., Picquet-Varrault, B., and Wallington, T. J.: Database for the
467   kinetics of the gas-phase atmospheric reactions of organic compounds, Earth Syst. Sci. Data, 12, 1203–1216,
468   https://doi.org/10.5194/essd-12-1203-2020, 2020.
469

470   Newland, M. J., Rea, G. J., Thüner, L. P., Henderson, A. P., Golding, B. T., Rickard, A. R., Barnes, I., and Wenger, J.:
471   Photochemistry of 2-butenedial and 4-oxo-2-pentenal under atmospheric boundary layer conditions, Phys. Chem. Chem. Phys.,
472   21, 1160-1171, 2019.
473

474   Novelli, A., Cho, C., Fuchs, H., Hofzumahaus, A., Rohrer, F., Tillmann, R., Kiendler-Scharr, A., Wahner, A., and Vereecken,
475   L.: Experimental and theoretical study on the impact of a nitrate group on the chemistry of alkoxy radicals, 23, 5474-5495, 2021.
476

477   Parrish, D. D., Lamarque, J. F., Naik, V., Horowitz, L., Shindell, D. T., Staehelin, J., Derwent, R., Cooper, O. R., Tanimoto, H.,
478   Volz-Thomas, A., Gilge, S., Scheel, H. E., Steinbacher, M. and Fröhlich, M.: Long-term changes in lower tropospheric baseline
479   ozone concentrations: Comparing chemistry-climate models and observations at northern midlatitudes, J. Geophys. Res., 119,
480   5719–5736, doi:10.1002/2013JD021435, 2014.
481

482   Ródenas, M: software for analysis of Infrared spectra. EUROCHAMP-2020 project, 2018. Available at
483   https://data.eurochamp.org/anasoft
484

485   Roman-Leshkov, Y., Barrett, C. J., Liu, Z. Y., and Dumesic, J. A.: Production of Dimethylfuran for Liquid Fuels from Biomass-
486   derived Carbohydrates, Nature, 447, 982−985, 2007.
487

488   Smith, D. F., McIver, C. D., and Kleindienst, T. E.: Primary product distribution from the reaction of hydroxyl radicals with
489   toluene at ppb NOx mixing ratios, J. Atmos. Chem., 30, 209–228, 1998.
490

491   Smith, D. F., Kleindienst, T. E., and McIver, C. D.: Primary Product Distributions from the Reaction of OH with m-, p-Xylene,
492   1,2,4- and 1,3,5-Trimethylbenzene, J. Atmos. Chem., 34, 339–364, 1999.
493

17

494 Sommariva, R., Cox, S., Martin, C., Borońska, K., Young, J., Jimack, P. K., Pilling, M. J., Matthaios, V. N., Nelson, B. S.,
495 Newland, M. J., Panagi, M., Bloss, W. J., Monks, P. S., and Rickard, A. R.: AtChem (version 1), an open-source box model for
496 the Master Chemical Mechanism, Geosci. Model Dev., 13, 169–183, https://doi.org/10.5194/gmd-13-169-2020, 2020.

498 Stewart, G. J., Acton, W. J. F., Nelson, B. S., Vaughan, A. R., Hopkins, J. R., Arya, R., Mondal, A., Jangirh, R., Ahlawat, S.,
499 Yadav, L., Sharma, S. K., Dunmore, R. E., Yunus, S. S. M., Hewitt, C. N., Nemitz, E., Mullinger, N., Gadi, R., Sahu, L. K.,
500 Tripathi, N., Rickard, A. R., Lee, J. D., Mandal, T. K., and Hamilton, J. F.: Emissions of non-methane volatile organic compounds
501 from combustion of domestic fuels in Delhi, India, Atmos. Chem. Phys., 21, 2383–2406, https://doi.org/10.5194/acp-21-2383-
502 2021, 2021a.

504 Stewart, G. J., Nelson, B. S., Acton, W. J. F., Vaughan, A. R., Hopkins, J. R., Yunus, S. S. M., Hewitt, C. N., Nemitz, E.,
505 Mullinger, N., Gadi, R., Rickard, A. R., Lee, J. D., Mandal, T. K., and Hamilton, J. F.: Comprehensive organic emission profiles,
506 secondary organic aerosol production potential, and OH reactivity of domestic fuel combustion in Delhi, India, Environ. Sci.:
507 Atmos., https://doi.org/10.1039/D0EA00009D, online first, 2021b.

509 Stone, D., Whalley, L., and Heard, D.: Tropospheric OH and HO_2 radicals: field measurements and model comparisons, Chem.
510 Soc. Rev., 41, 6348-6404, 2012.

512 Wang, J. J., Liu, X. H., Hu, B. C., Lu, G. Z., Wang, Y. Q.: Efficient Catalytic Conversion of Lignocellulosic Biomass into
513 Renewable Liquid Biofuels via Furan Derivatives. RSC Adv., 4, 31101− 31107, 2014.

515 Whelan, C. A., Eble, J. Mir, Z. S., Blitz, M. A., Seakins, P. W., Olzmann, M., and Stone D.: Kinetics of the Reactions of Hydroxyl
516 Radicals with Furan and Its Alkylated Derivatives 2-Methyl Furan and 2,5-Dimethyl Furan, *J. Phys. Chem. A*, 124, 7416–7426,
517 2020.

519 Wyche, K. P., Monks, P. S., Ellis, A. M., Cordell, R. L., Parker, A. E., Whyte, C., Metzger, A., Dommen, J., Duplissy, J., Prevot,
520 A. S. H., Baltensperger, U., Rickard, A. R., and Wulfert, F.: Gas phase precursors to anthropogenic secondary organic aerosol:
521 detailed observations of 1,3,5-trimethylbenzene photooxidation, Atmos. Chem. Phys., 9, 635–665, https://doi.org/10.5194/acp-
522 9-635-2009, 2009.

524 Yuan, Y. Zhao, X., Wang, S., and Wang, L: Atmospheric Oxidation of Furan and Methyl-Substituted Furans Initiated by
525 Hydroxyl Radicals, J. Phys. Chem. A, 121, 9306-9319, 2017.